Journal of
Materials Chemistry C

This article can be cited before page numbers have been issued, to do this please use: T. Singha Mahapatra, H. Singh, A. Maity, A. Dey, S. K. Pramanik, E. Suresh and A. Das, *J. Mater. Chem. C*, 2018, DOI: 10.1039/C8TC03487G.

DOI: 10.1039/C8TC03487G

Journal Name

ARTICLE

White-Light-Emitting Lanthanide and Lanthanide-Iridium Doped Supramolecular Gels: Modular Luminescence and Stimuli-Responsive Behaviour

Received 00th January 20xx,
Accepted 00th January 20xx

DOI: 10.1039/x0xx00000x

www.rsc.org/

Tufan Singha Mahapatra,*[a] Harwinder Singh,[a] Arunava Maity,[a] Ananta Dey,[a] Sumit Kumar Pramanik,[a] Eringathodi Suresh[a] and Amitava Das*[a]

Light-emitting materials are of significant interest owing to their potential applications in electroluminescent devices/ displays and sensors. Herein, light-emitting metallogel systems are developed using self-assembled Ln(III)-complexes (Ln(III) = Eu(III) and Tb(III)) of 4′-p-fluorophenyl-2,2′:6′,2′′-terpyridine (L-F) and 4′-p-chlorophenyl-2,2′:6′,2′′-terpyridine (L-Cl) ligands. The luminescence of these metallogels could be tuned over a wide spectrum. A near-white light emission (CIE coordinates: (0.31, 0.36) and (0.34, 0.36)) was achieved by controlling the [L-X] (X= F, Cl)/[Eu(III)]/[Tb(III)] stoichiometry. Adopting an alternate strategy, near white light emission was also achieved using metallogel derived from Eu•L-F-Ir (CIE coordinates: 0.28, 0.35) and Eu•L-Cl-Ir (CIE coordinates: 0.31, 0.35). For this, a blue emissive [$Ir^{III}(F_2ppy)_2(biimid)]PF_6$ complex was used along with Eu(III)-terpyridine gel systems (red emissive component). Eu•L-F, Tb•L-F and Eu•L-F-Ir (1 wt%) could also be incorporated into poly(methyl methacrylate) (PMMA) polymer matrix for developing transparent red, green and white luminescent PMMA films with excellent UV-shielding properties. Being colourless to the naked eye and luminescent on exposure to a UV-irradiation, such metallogels have the potential to be used as an invisible security ink. Moreover, dynamic nature of Ln−N(terpyridine) coordination bonds was utilized for demonstrating the chemo/ vapor-responsive behaviour of the lanthanide-based gel systems, which could offer a suitable pathway for future engineering of stimuli-responsive gel materials.

Introduction

Supramolecular gels derived from small molecules are commonly known as low molecular weight gelators (LMWGs). Such LMWGs have captivated great interest across various research disciplines owing to their potential applications as biomaterials, smart or adaptive materials, color tuneable displays, chemical sensors, electronic materials, and in many such associated fields.[1-12] In an appropriate solvent system, individual gelator molecules could self-assemble to form an entangled network by participating in multiple non-covalent interactions, such as hydrogen bonding, van der Waals interactions, π···π stacking interactions, CH···π interaction, hydrophobic-hydrophobic interactions etc., and a combination of such interactions eventually induce a sol to gel transformation.[13-17] Appropriate choice of the metal ions, coordinating ligand(s) and metal-ligand coordination offer an option for introducing optical or/and physicochemical properties into the LMWGs that are typical for the metal-ligand complex system. Lately, luminescent supramolecular metallogels have been explored by various researchers where metallogels are derived from Eu(III) and Tb(III) ions for achieving an interesting light emitting properties. Key features of the emission property of such gels include sharp and well-defined emission bands, long luminescent lifetimes (in the millisecond range), relatively high emission quantum yields and less sensitivity towards emission quenching through the vibrational energy transfer of the surrounding ligand systems.[2,8,18-28] Recent reports on lanthanide (Ln^{III})-based luminescent gels by Gunnlaugsson,[18-20] Holten-Andersen,[2,48] Liu,[8] Maitra,[21,22] Maji,[23,24,27,28] Jung,[25] and their co-workers have discussed LMWGs that show various material properties, including tuneable luminescence and white light emission. White-light-emitting materials usually are comprised of single or multiple components that can emit either the three primaries (red, green, and blue) or two complementary (orange and turquoise) colors.[11] Using lanthanide-based complexes, white light emitting systems are contrived by mixing red emissive Eu(III) and green emissive Tb(III) in an appropriate ratio in combination with a blue emissive ligand.[2,23,24,28-30] De Cola,[31] Ward et al.[32,33] and their collaborators have elegantly demonstrated that using appropriate Ir^{III}-Eu^{III} based dyads, a delicate balance between Ir(III)-based blue emission and the sensitized Eu(III)-based red emission could be achieved for

---

[a] *Analytical and Environmental Science Division and Centralized Instrument Facility, CSIR-Central Salt & Marine Chemicals Research Institute, Bhavnagar 364002, Gujarat, India. *E-mail: tufansmp@gmail.com, a.das@csmcri.res.in*

Electronic Supplementary Information (ESI) available: [details of any supplementary information available should be included here]. See DOI: 10.1039/x0xx00000x

View Article Online
DOI: 10.1039/C8TC03487C

generating the white light. Despite such advances, reports on Ln^{III}-Ir^{III} doped white emissive metallogels are scanty in literature. There are examples of white light generation using organic molecules as LMWG. However, relative instability of the photo-excited state and subsequent photo-bleaching on irradiation have restricted the use of such material for device application.[34-37]

The supramolecular gel that alters its phase, photophysical properties and/or morphology in responses to some external stimuli such as light, temperature, pH, molecular/ionic input, etc. has significance in contemporary research for developing stimuli-responsive smart gels. Among the various stimuli-responsive materials, lanthanide-based gels with dynamic metal-ligand coordination have significance primarily due to the ease of synthesis of Ln(III)-terpyridyl complexes, their tuneable luminescence behaviour, and stable photo-excited states. Such tunable and stimuli-responsive gels are important for diverse applications, including energy efficient luminescent displays, imaging probes, molecular receptors, and metal-controlled photo-modulation properties.[2,38-42] Although there are literature reports on stimuli-responsive (thermo-, mechano-, photo-, and chemo-responsive) organogels or hydrogels,[43-47] reports on lanthanide-based gels are rather limited.[2,24,48]

Herein, we have discussed unique gelation properties of two different derivatives of 4′-p-halophenyl-2,2′:6′,2′′-terpyridine (L-X, X= F, Cl) (Fig. 1). The choice of the terpyridine moiety is based on its demonstrated ability to act as a light-harvesting antenna for sensitization of the Ln(III) ion.[49] The gelation propensity of the terpyridine ligands (L-X) in the presence of Eu(III) and Tb(III) are explored to obtain bright red and green emissive gels, respectively. The optical properties of these gel systems could be tuned by modulating the stoichiometric ratio of [Eu(III)]:[Tb(III)] to obtain yellow and near white emissions. White light emission is also achieved by doping either red emissive Eu•L-Cl or Eu•L-F gel system with an appropriate blue emissive complex, $[Ir^{III}(F_2ppy)_2(biimid)]PF_6$. All the metallogels are comprised of entangled fibrous networks as evident from FESEM micrographs. Furthermore, we have explored the reversible chemo/ vapor-responsive properties of the lanthanide-based gels by utilizing the dynamic coordination behaviour of the terpyridyl moiety of L-X towards Eu(III)/Tb(III) ions. Being colourless to the naked eye and luminescent on exposure to a UV-irradiation, such metallogels have the potential to be used as an invisible security ink. In addition, we have successfully prepared luminescent films by simple drop casting of Ln•L-F (Ln is Eu^{III} or Tb^{III}) solutions on transparent agarose gel support or by incorporating Ln•L-F or Eu•L-F-Ir into the poly(methyl methacrylate) (PMMA) polymer matrix without amending the optical properties of the metallogels. The results from UV-transmittance spectra indicate that the Ln•L-F-PMMA and Eu•L-F-Ir-PMMA films could be used as a novel UV absorber for developing transparent UV-shielding film.

Results and discussion

Synthesis and gelation property of L-X ligands (X = F and Cl)

Terpyridine derivatives, 4′-p-fluorophenyl-2,2′:6′,2′′-terpyridine (L-F) and 4′-p-chlorophenyl-2,2′:6′,2′′-terpyridine (L-Cl) were synthesized following previously reported procedures.[50,51] Condensation of 2-acetylpyridine with the appropriate p-halobenzaldehydes (Scheme S1) yielded the desired compounds. Following necessary purification procedures, each desired compound was isolated in pure form. The purity of each, the compound was ensured based on the results of the various spectroscopic (^{1}H NMR, HR-MS spectroscopy) and single crystal structural studies.

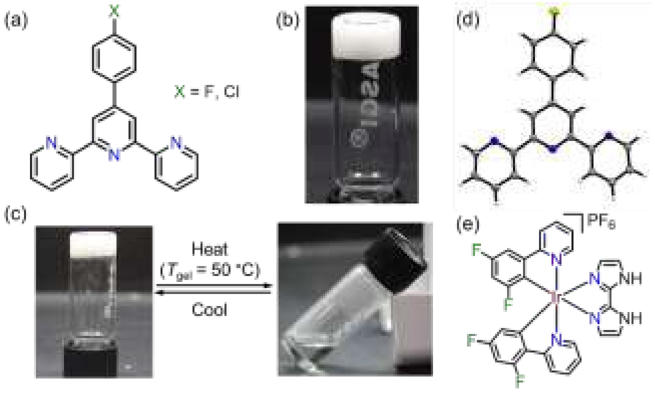

Fig. 1 (a) Molecular structure of L-X (X = F and Cl); (b) L-F gel under day light; (c) photographs displaying thermal reversibility of L-Cl gel (CGC is 1.6 wt% in MeCN); (d) ORTEP depiction of L-F showing 30% probability ellipsoids. Colour code: N, blue; C, grey; F, yellow and H, white; and (e) molecular structure of $[Ir^{III}(F_2ppy)_2(biimid)]PF_6$.

Synthesized terpyridine derivatives (L-F and L-Cl) formed thermoreversible (T_{gel} = 50 °C) white colour opaque gels in MeCN, MeCN/DMF (1:1, v/v) and DMF (Fig. 1a-d). Gel formation in each instance was subsisted with the inversion test and no mass flow was observed upon upending the glass vials (Fig. 1b). The critical gelation concentration (CGC) value was found to be 1.6 wt% in MeCN and MeCN/DMF (1:1, v/v) solvents, whereas in DMF solvent CGC was evaluated as 2.2 wt%. It was presumed that the self-assembly process of the terpyridyl derivatives L-F/L-Cl was induced typically by various hydrogen bonding (H-bonding) and intermolecular $\pi\cdots\pi$ stacking interactions among the respective terpyridyl moieties (L-X). This was further confirmed by single crystal X-ray structure and the analyses of the powder X-ray diffraction (PXRD) pattern. Interestingly, the fibers of L-F gel in MeCN/DMF (1:1, v/v) was transformed into X-ray quality crystalline rods when the gel was kept at room temperature for 14-18 days (Fig. 1d). The ligand was found to be crystallized in monoclinic $P2_1/c$ space group and selected metric parameters are summarized in Table S1. X-ray structure divulged that adjacent L-F molecules were connected through C–H⋯F (2.529 and 2.568 Å) and C–H⋯N (2.716 Å) H-bonding interactions and two layers were associated through face-to-face $\pi\cdots\pi$ stacking interactions between the aromatic moieties (intercentroid distance: 3.836 Å) (Fig. 2). The powder X-ray diffraction (PXRD) pattern of L-F xerogel was consistent with its simulated data, obtained from the single crystal X-ray diffraction data (.cif files) using the CCDC Mercury software (Fig. S1, ESI†). To realize the role of the halogen atom in terpyridine moiety, gelation test was performed using the model terpyridyl derivatives, 4′-p-methylphenyl-2,2′:6′,2′′-terpyridine (L-Me)

View Article Online
DOI: 10.1039/C8TC03487G

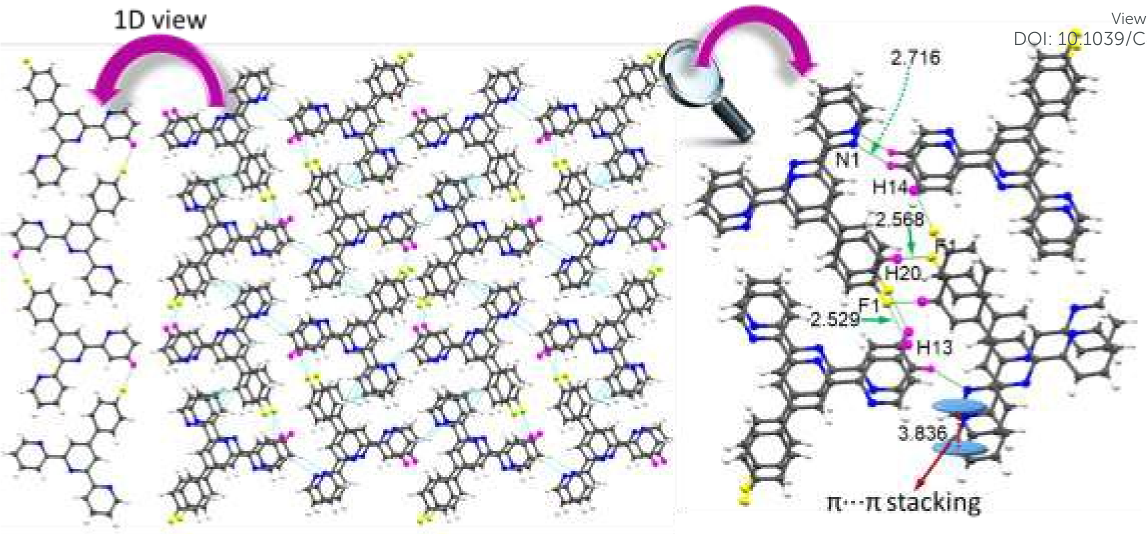

Fig. 2 Crystal structure of L-F showing the self-assembly through H-bonding and π···π stacking interactions, Colour code: N, blue; C, grey; F, yellow and H, white & pink (those involved in H-bonding interactions)

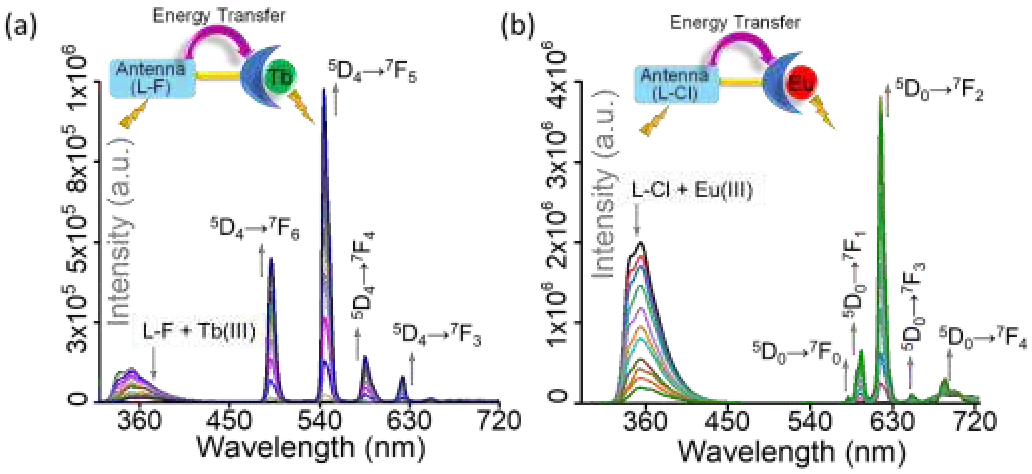

Fig. 3. Spectral changes in (a) the Tb(III) and (b) Eu(III) centred luminescence spectra upon titrating L-F or L-Cl (1.0×10^{-5} M) with Tb(III)/Eu(III) (0 → 1 mole equiv.) in MeCN. Insets: Representations for describing a mechanism for sensitized lanthanide (Eu^{III} or Tb^{III}) luminescence.

and 4′-p-hydroxyphenyl-2,2′:6′,2′′-terpyridine (L-OH) and no gel formation was observed (Scheme S2, ESI†). This further confirmed the significance of the C–H···X (X = F, Cl) H-bonding interactions that were otherwise operational for L-X derivatives.

Interaction of L-F/Cl with Tb/Eu(NO$_3$)$_3$·6H$_2$O in solution

The interaction of either of the two terpyridyl derivatives (L-F or L-Cl) with lanthanide ions (Tb(III) or Eu(III)) was investigated in MeCN solution at low concentration by monitoring the changes in the absorption and luminescence spectra of L-F/ L-Cl and Tb(III)/ Eu(III) centred emissions. The electronic spectrum of L-F/L-Cl in MeCN solution (1.0×10^{-5} M) consisted of two main bands centred at 252/253 nm ($\varepsilon^{L\text{-}F}$ = 31600 & $\varepsilon^{L\text{-}Cl}$ = 32400 L mol^{-1} cm^{-1}) and 276 nm ($\varepsilon^{L\text{-}F}$ = 29200 & $\varepsilon^{L\text{-}Cl}$ = 33760 L mol^{-1} cm^{-1}). Both bands were predominantly due to terpyridine-based π→π* transitions (Fig. S2, ESI†). Electronic spectra were also recorded for the acetonitrile solution of L-F/L-Cl in presence of varying concentration (0 - 1 mole equiv.) of Tb(III) or Eu(III). Spectral changes were almost identical for both L-F and L-Cl and a red shift was observed for the 276 nm band. A new sharp band appeared at around 289 nm for both Tb(III) and Eu(III), indicating the formation of the respective Tb^{III}•L-F, Tb^{III}•L-Cl, Eu^{III}•L-F and Eu^{III}•L-Cl complexes (Fig. S2, ESI†, *vide infra*). The steady state luminescence spectrum ($\lambda_{ex}^{L\text{-}F}$ or $\lambda_{ex}^{L\text{-}Cl}$: 285 nm) of L-F and L-Cl in MeCN solution (1.0×10^{-5} M) exhibited strong emission band maxima at 352 and 355 nm, respectively, which were associated with terpyridine-based π→π* transitions. With the incremental addition (0 - 1 mole equivalents) of Tb(III) to the L-F solution, a decrease in luminescence intensity of the ligand centred emission band at 352 nm with the concomitant emergence of sharp bands at 491 nm, 544 nm, 585 nm, and 623 nm, respectively, were observed. These emission bands were assigned to $^5D_4 \rightarrow {}^7F_6$, $^5D_4 \rightarrow {}^7F_5$, $^5D_4 \rightarrow {}^7F_4$, and $^5D_4 \rightarrow {}^7F_3$ based transitions, respectively, for Tb(III) (Fig. 3a). The similar trend was observed upon addition of Eu(III) (0 - 1 mole equivalents) to the L-Cl (1.0×10^{-5} M in MeCN) with the occurrence of five characteristics Eu(III)-based emission bands having maxima at

View Article Online
DOI: 10.1039/C8TC03487G

581 nm ($^5D_0 \rightarrow {}^7F_0$), 596 nm ($^5D_0 \rightarrow {}^7F_1$), 617 nm ($^5D_0 \rightarrow {}^7F_2$), 651 nm ($^5D_0 \rightarrow {}^7F_3$), and 687 nm ($^5D_0 \rightarrow {}^7F_4$) (Fig.3b). This sensitized emission was a direct consequence of the binding of Tb(III) or Eu(III) to the respective terpyridine based ligands (L-F/L-Cl) (Fig. 3 and Fig. S3, ESI†). Upon irradiation with a suitable wavelength, the short-lived singlet electronically excited state ($S_o \rightarrow S_1$) of the terpyridine moiety was populated and this subsequently underwent intersystem crossing (ISC) for generating the longer-lived lower lying triplet excited state (T_1). Next, sensitization happens by populating the excited state $^5D_0$ of Eu(III) and $^5D_4$ of Tb(III) through energy transfer from the T_1 state of the terpyridine with subsequent deactivation to the ^7F_J ground states, which accounted for the characteristic emission bands (Scheme S3, ESI†).[49] Respective binding constants was evaluated using Benesi-Hildebrand (B–H) plots for the formation of complexes between L-X (X = F, Cl) and Tb(III)/Eu(III): $K^{L\text{-}F/Tb(III)} = 7.56 \pm 0.22 \times 10^4$ and $K^{L\text{-}Cl/Eu(III)} = 2.43 \pm 0.14 \times 10^4$ (Fig. S4, ESI†). A good linear fit of the B-H plot also supports the 1:1 (M:L) binding stoichiometry.[52,53]

Formation of metal-based gels from L-F/L-Cl and their photophysical properties

The gelation propensity of L-X (X = F, Cl) in presence of respective Eu(III) and Tb(III) ions was explored in DMF solvent. The lanthanide-based gels were obtained by mixing solutions containing a 1:1 molar ratio of L-X and $Eu(NO_3)_3{\cdot}6H_2O$ or $Tb(NO_3)_3{\cdot}6H_2O$. Formation of coordinated Eu(III) and Tb(III) in corresponding Eu•L-X and Tb•L-X xerogels was confirmed from the results of the FT-IR and luminescence spectral studies. The presence of the coordinated nitrato group in Eu•L-F and Tb•L-F xerogels was confirmed by the characteristic asymmetric stretching (ν_{ONO}) frequency at 1382 cm^{-1} in the FT-IR spectra (Fig. S5a, ESI†). Eu/Tb-terpyridyl coordination presumably prevails in the formation of Eu•L-X/Tb•L-X involving L-X ligand.[2,23,24] Coordination of six O-atoms from the three bidentate nitrate ions is also proposed (Scheme S4, ESI†).[54-57] To gain insight into the molecular packing of these lanthanide gels PXRD patterns of the air-dried gels were recorded. PXRD patterns of Eu•L-F and Tb•L-F gels were exhibited peaks at higher 2θ values 16.46, 16.98, 17.73, 19.64 and 25.74 with respective d-spacing values of 5.38 Å, 5.22 Å, 4.99 Å, 4.52 Å, and 3.50 Å (Fig. S5b, ESI†). Peaks at 2θ = 25.74 with d-spacing values 3.50 Å suggested the presence of intermolecular π···π stacking interactions in metallogels,[6] which confirmed the formation of higher order self-assembled supramolecular structure in those metallogels (Scheme 1).

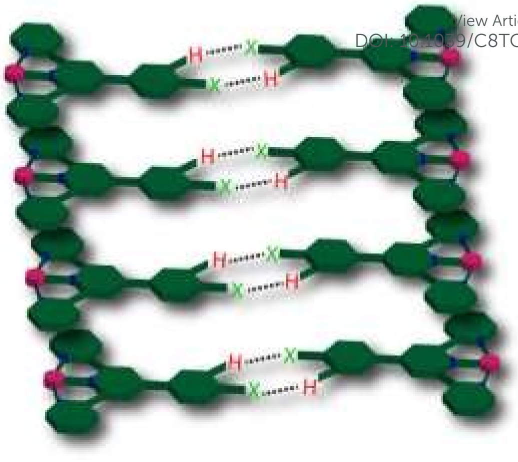

Scheme 1. Schematic showing the probable self-assembled supramolecular structure in Eu•L-X and Tb•L-X gels (X= F, and Cl). Colour Code: N, blue; C, green; Eu/Tb, pink.

The individual gels showed bright red (Eu•L-X) and green (Tb•L-X) fluorescence upon exposure to UV light irradiation at 365 nm (Fig. 4). The colour perceptions of each individual gel were further analyzed using the CIE (Commission International de L'Eclairage) chromaticity diagram.

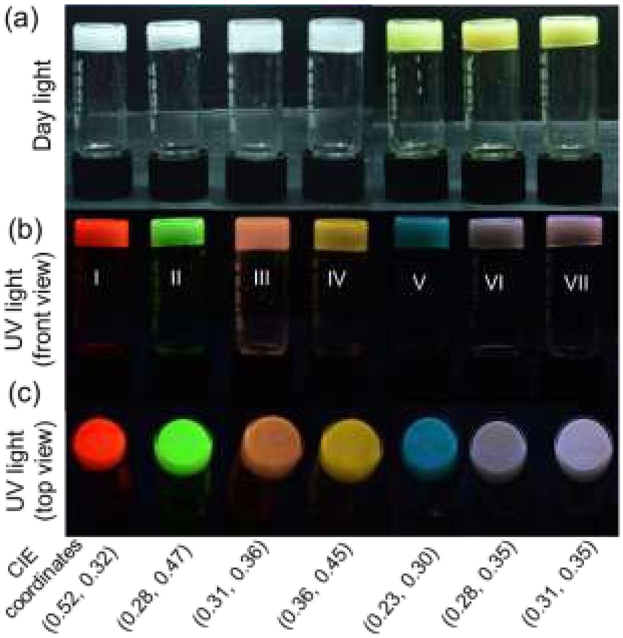

Fig. 4 Photographs of metallogels (a) in day light and (b & c) their respective luminescence under UV light irradiation (λ_{ex} = 365 nm). Corresponding CIE coordinates are mentioned below. I: Eu•L-F, II: Tb•L-F, III: Eu•L-F-Tb•L-F, IV: Eu•L-F-2(Tb•L-F), V: Ir-L-F, VI: Eu•L-F-Ir, and VII: Eu•L-Cl-Ir.

The emission spectrum (λ_{ex} = 285 nm) of the Eu•L-F gel (CIE coordinates: 0.52, 0.32) exhibited characteristics sharp

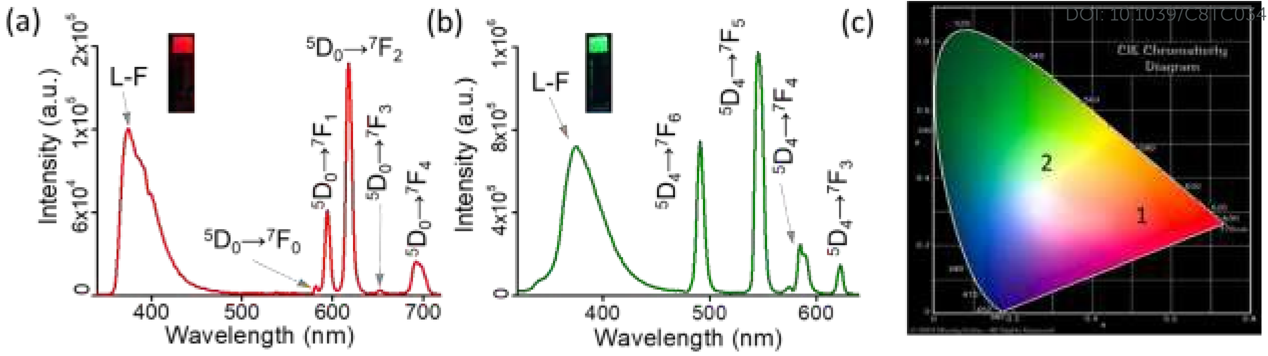

Fig. 5. Luminescence spectra of (a) Eu•L-F and (b) Tb•L-F gels obtained from DMF; (c) CIE chromaticity diagram of Eu•L-F (1) and Tb•L-F (2)

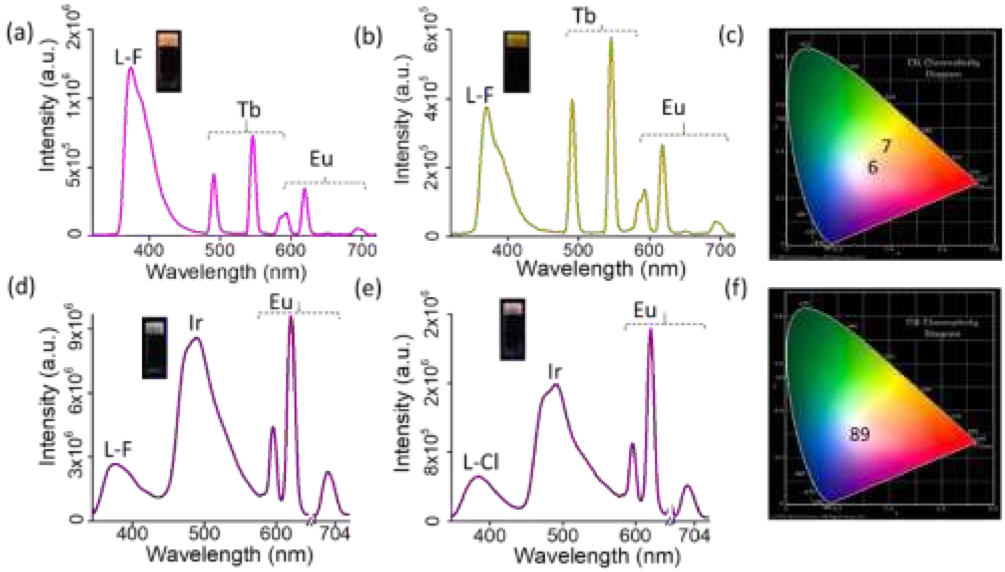

Fig. 6 Luminescence spectra of respective gel: (a) Eu•L-F-Tb•L-F, (b) Eu•L-F-2(Tb•L-F), (λ_{ex} = 285 nm), (d) Eu•L-F-Ir and (e) Eu•L-Cl-Ir (λ_{ex} = 330 nm). Insets: Photographs of corresponding gels under UV light. (c and f) CIE chromaticity diagram of Eu•L-F-Tb•L-F (6), Eu•L-F-2(Tb•L-F) (7), Eu•L-F-Ir (8) and Eu•L-Cl-Ir (9). Note: (d and e) Axis-Break from 645-675 to cut-off the peak at twice the excitation wavelength (λ_{ex} = 330 nm) due to 2nd-order transmission.

emission bands for Eu(III) at 582, 594, 617, 652, and 693 nm, which were associated with $^5D_0 \rightarrow {}^7F_J$ (J = 0–4) based transitions and a ligand centred band with maximum at 374 nm (Fig. 5a,c). Likewise, Tb•L-F gel (CIE coordinates: 0.28, 0.47) displayed sharp bands for Tb(III) at 491, 545, 584 and 622 nm and were assigned to $^5D_4 \rightarrow {}^7F_J$ (J = 6–3) based transitions (Fig. 5b,c). The same overall trend was observed in the emission spectra of Eu•L-Cl (CIE coordinates: 0.44, 0.30) and Tb•L-Cl (CIE coordinates: 0.27, 0.42) gels (Fig. S6a,b, and S7, ESI†).

The entire visible spectrum (400–750 nm) can be covered using the red, green, and blue (RGB) mixing approach. To accomplish this, the emission properties of mixed metallogels were investigated further by mixing both Eu(III) and Tb(III) to L-X in different stoichiometry in DMF solvent. However, in all such mixed metallogels, [L-X]:[Ln] ([Ln] = [Eu] + [Tb]) ratio was fixed at 1:1. Interestingly, mixed Eu•L-F-Tb•L-F gel obtained by mixing the equimolar amount of Eu(III) and Tb(III) into L-F in DMF solvent, exhibited almost white light emission (CIE coordinates: 0.31, 0.36) (Table 1 and Fig. 6a,c and 4). Similar was the observation for Eu•L-Cl-Tb•L-Cl, (CIE coordinates: 0.34, 0.36). These coordinates were close to that of pure white light (0.33, 0.33). (Fig. S6c and S7, ESI†). The emission spectra (λ_{ex} = 285 nm) of these mixed Eu•L-X-Tb•L-X gels cover the entire visible spectrum with characteristic bands from ligand, Tb(III) at 491, 545 and 584 nm (green) and Eu(III) at 594, 617, 652 and 693 nm (red) (Fig. 6a,c), which presumably accounted for the observed white light emission. Whereas, the Eu•L-F-2(Tb•L-F) gel (Eu(III):Tb(III) = 1:2) obtained from DMF solvent exhibited yellow emission (CIE coordinate: 0.36, 0.45) upon exposure to UV light (λ_{ex} = 285 nm, Table 1, Fig. 6b,c and 4). Similarly, yellow emission was observed from Eu•L-Cl-2(Tb•L-Cl) (CIE coordinates: 0.30, 0.41) (Fig. S6d and S7, ESI†). In all of these metallogels, L-X acted as a sensitizer for both Eu(III) and Tb(III) centres. A combination of emissions that originated from L-X, Eu(III) and Tb(III) in appropriate ratio accounted for the eventual white emission. A modification of the ratio of the three emissive components helped in achieving tuneable luminescent metallogels. However, a possibility of partial energy transfer from Tb(III) to the Eu(III) centre cannot be completely ruled out.[22,28,29]

White light can also be created by combining a blue emitting Ir(III) component to the sensitized red emission of the Eu(III) component. With this rationale, we synthesized a mononuclear $[Ir^{III}(F_2ppy)_2(biimid)]PF_6$ complex (Fig. 1e) using 2,2´-biimidazole (biimid) (2.4 eq) and Ir(III)-dimer complex, $[(F_2ppy)_2Ir(\mu\text{-}Cl)]_2$ (1 eq) following a literature procedure with necessary modification (Scheme S5, ESI†).[58] This complex was characterized by ^1H NMR and HR-MS spectroscopy. The complex displayed emission in blue region with two band maxima at 459 and 484 nm (λ_{ex} = 385 nm) in MeCN (1.0×10^{-5} M) (Fig. S8a, ESI†). Next, a definite amount of this blue emitting $[Ir^{III}(F_2ppy)_2(biimid)]PF_6$ (Ir) complex was doped into red emitting Eu•L-F/ Eu•L-Cl gel component and the assembly (Eu•L-F-Ir/ Eu•L-Cl-Ir gel) showed a nearly white light emission (Fig. 4). The CIE coordinates of the corresponding gels were evaluated (Eu•L-F-Ir: 0.28, 0.35 and Eu•L-Cl-Ir: 0.31, 0.35) and these values were close to that of pure white light (0.33, 0.33) (Fig. 6f). The emission spectra of Eu•L-F-Ir/ Eu•L-Cl-Ir (λ_{ex} = 330 nm) gel displayed ligand centred band at 374 (L-F) or 384 nm (L-Cl), a broad band at 490 nm (blue-green region) from $Ir^{III}(F_2ppy)_2(biimid)]^+$ and three sharp bands at 595, 620, and 695 nm (red region) that were characteristic of the Eu(III)-centred emissions (Fig. 6d,e). This eventually covered the entire visible spectrum and resulted in a white-light emission. We also prepared blue emitting Ir-L-X gels by doping $[Ir^{III}(F_2ppy)_2(biimid)]PF_6$ into the L-X gel component (Fig. 4). Luminescence spectrum of Ir-L-F gel supported the blue emission (CIE coordinates: 0.23, 0.30) with a broad band at 490 nm (Fig. S8b, ESI†).

Table 1. Photophysical properties of mixed gels obtained from DMF solvent.

Mixed gels	[L-X]:[Ln] ([Ln]= [Eu]+[Tb])	[Eu]:[Tb]	Emission colour	CIE coordinates
Eu•L-F-Tb•L-F	1:1	1:1	Near white	0.31, 0.36
Eu•L-F-2(Tb•L-F)		1:2	Yellow	0.36, 0.45
Eu•L-Cl-Tb•L-Cl		1:1	Near white	0.34, 0.36
Eu•L-Cl-2(Tb•L-Cl)		1:2	Yellow	0.30, 0.41

Optical applications

These soft gels are also well suited for generating coated surfaces or thin-films. We have applied these gels on a nonfluorescent glass plate to print 'CSIR-CSMCRI' having blue, green, yellow, orange, and red-light emission under UV light with excellent colour quality using different combinations of the gels discussed in the previous section (Fig. S9a, ESI†). Next, we have written 'CSMCRI' on a silica gel plate using Eu•L-F gel which remained colourless and imperceptible to the naked eye on irradiation with normal visible light. However, under UV light irradiation (λ_{ex} = 365 nm) the alphabets emitted red light and became visible (Fig. S9b, ESI†). This demonstrates the possibility of using such gel for security purposes, where gel materials can be used as an invisible security ink for writing secret codes. With an intention to fabricate optical materials having moderate luminescence and option for easy colour tunability, we have prepared luminescent films on transparent agarose gel support by simple drop casting of the lanthanide sols on freshly prepared agarose gel. The snapshots of the Eu•L-F, Tb•L-F, Eu•L-F-Tb•L-F and Eu•L-F-2(Tb•L-F) coated-agarose gel showed red, green, white and yellow light emission (λ_{ex} = 365 nm), respectively, with decent colour quality (Fig. S9c-f, ESI†). Interestingly, it was also possible to bend the coated films without losing any emission intensity of the resulting films (Fig. S9c-f, Inset, ESI†).

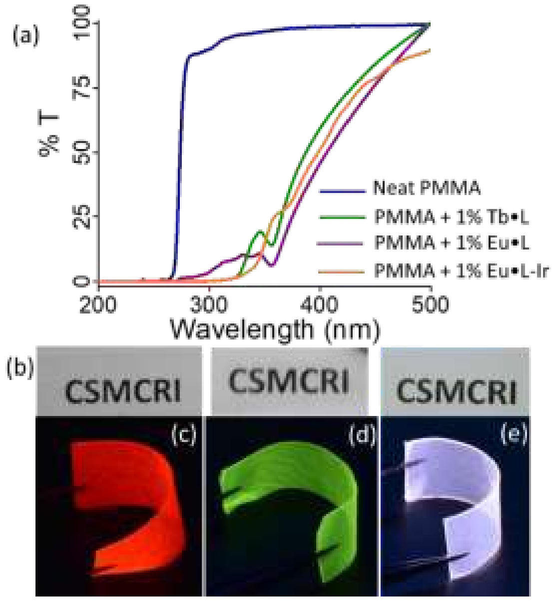

Fig.7 (a) The UV–vis transmittance spectra of neat PMMA, Eu•L-F-PMMA, Tb•L-F-PMMA and Eu•L-F-Ir-PMMA films. (b) Eu•L-F-PMMA, Tb•L-F-PMMA and Eu•L-F-Ir-PMMA films placed over a printed script 'CSMCRI' depicting the transparency of the film in daylight and (c) Eu•L-F-PMMA, (d) Tb•L-F-PMMA, (e) Eu•L-F-Ir-PMMA films under UV light irradiation after bending.

Further, PMMA/Ln•L-F composite films were prepared by following casting method. Poly(methyl methacrylate) (PMMA) was dissolved in toluene and then Eu•L-F or Tb•L-F or Eu•L-F-Ir sols (1 wt%) was added under stirring condition. Homogeneous solution was casted on a petri dish for solvent evaporation and subsequently dried in a vacuum oven to achieve respective colourless transparent film (Fig. 7b), which emitted red (Eu•L-F-PMMA) or green (Tb•L-F-PMMA) or white (Eu•L-F-Ir-PMMA) on exposure to an UV-irradiation (Fig. 7c-e). Prepared films were flexible and could be folded to provide different shapes with retention of their optical properties (Fig. 7c-e). PMMA was chosen as a matrix due to its transparent thermoplastic nature which often used as a shatterproof substitute for glass. Interestingly, these transparent hybrid films displayed notable UV-shielding properties. UV–vis transmittance spectra of Eu•L-F-PMMA, Tb•L-F-PMMA and Eu•L-F-Ir-PMMA hybrid films showed that the transmitting efficacy of the films was very less in UV region up to 360 nm, which supported their excellent UV cut-off performance (Fig. 7a). Thus, these hybrid films have potential application in UV-shielding glasses and window films. The solid-state emitting capabilities and easy material processabilities of these gel materials can be exploited for other

View Article Online
DOI: 10.1039/C8TC03487G

probable optical applications such as the production of coated light-emitting diodes (LED), specific secret barcode systems and thin-films for use in tamper seals.

Morphological properties of gels

The morphologies of the gels were examined by recording field emission scanning electron microscopic (FESEM) images of the corresponding xerogel to gain insight into the self-assembly process. The FESEM micrographs of L-F xerogel in DMF demonstrated the formation of multi brunched entangled tree like fibrous network with fibre at about micrometer in length and width ranging from ~ 390 - 820 nm (Fig. 8a). The corresponding metallo xerogels (Eu•L-F, Tb•L-F, Eu•L-F-Tb•L-F, Ir-L-F, and Eu•L-F-Ir) in DMF showed a similar type of fibrous network in FESEM micrograph (Fig. 8c-g). In comparison to the fibers of L-F (~ 390 - 820 nm), the fibres obtained from metallogels were thick in nature (~ 0.95–3.94 µm).

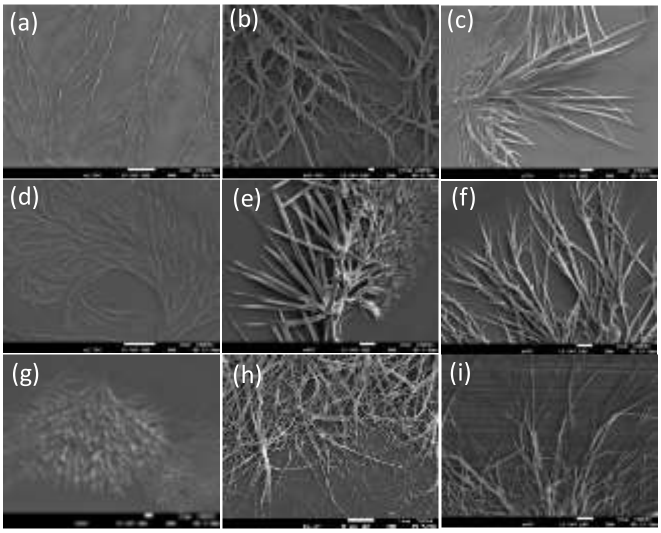

Fig. 8 FESEM micrographs of (a) L-F xerogel showing multi brunched tree like fibrous network, (b) L-Cl xerogel showing network of helical fibers, (c-i) Eu•L-F, Tb•L-F, Eu•L-F-Tb•L-F, Ir-L-F, Eu•L-F-Ir, Eu•L-Cl, and Tb•L-Cl metallo xerogels showing fibrous structures.

L-Cl xerogel in DMF unveiled a network of helical fibres, comprised of thin fibres of nanometer diameter (100 - 200 nm) and micrometer in length (Fig. 8b). Presumably, the observed helical nature of the fibers occurred due to the interwinding of thin fibers during the assembly process. However, FESEM images of Eu•L-Cl and Tb•L-Cl xerogel showed simple fibers instead of helical fibers that were observed in the L-Cl gel (Fig. 8h,i). Energy-dispersive X-ray spectroscopy (EDXS) analysis confirmed the presence of Eu(III), Tb(III) and Ir(III) in the above-mentioned xerogels.

Fluorescence microscopy also revealed that the respective gel of Eu•L-F, Tb•L-F, Eu•L-F-2(Tb•L-F) and Ir-L-F was composed of red, green, yellow and blue light-emitting self-assembled fibres (Fig. S10, ESI†).

Rheological properties of gels

Rheological experiments (strain and frequency sweeps) were performed for investigating the mechanical properties of these supramolecular gels (Fig. 9 and Fig. S11, ESI†). The oscillatory strain sweep measurements for all the gels exhibited nonlinear behaviour of the storage modulus (G′, the contribution of elastic) and loss modulus (G″, the contribution of viscous) to a fixed frequency (f = 1 Hz) by varying the strain amplitude (Fig. 9a,b,c). At low strain amplitudes, the storage modulus remained constant and the response was solid-like (G′ > G″). However, after reaching the yield strain, G′ was decreased rapidly, suggesting that the gel network was collapsed and became sol. After determination of linear viscoelastic region by strain-sweep measurements, frequency sweep measurements were performed. All the gels showed little frequency dependence of the storage modulus (G′) to a fixed small amplitude of strain (0.1%). G′ exceeded G′′ by almost an order of magnitude in all the cases, thereby suggesting elastic nature of the gels (Fig. 9d,e,f and Fig. S11, ESI†). While the overall behaviour of the G′ and G′′ were similar for all the gels, the G′ of metallogels (Tb•L-F, Eu•L-F, Eu•L-F-Tb•L-F and Eu•L-F-Ir) were an order of magnitude larger compared to the G′ of the ligand gel (L-F). This confirms higher rigidity of metallogels compared to L-F gel. Moreover, mixed Eu•L-F-Tb•L-F and Eu•L-F-Ir gels were found to be softer compared to the pure Tb•L-F and Eu•L-F gels.

Stimuli-responsiveness of the metallogels

We explored stimuli-responsive properties of the red emitting Eu•L-F and mixed metal white light emitting Eu•L-F-Tb•L-F gels. Upon exposure to the vapor of trifluoroacetic acid (TFA), a distinct gel-to-sol transition was observed with subsequent change in emission spectra (Fig. 10a,b). This phenomenon was ascribed to the dissociation of the Ln(III)-terpyridyl complexes, which was induced by the diffusion of TFA vapor into the gel matrix and the subsequent protonation of the nitrogen atoms of the terpyridine ligand. The corresponding emission spectrum of the TFA exposed Eu•L-F-Tb•L-F sol displayed a broad band at 435 nm, attributed to the free protonated terpyridine ligand (Fig. 10b). Similarly, TFA exposed Eu•L-F sol displayed a broad band at 436 nm with the low-intensity Eu(III)-centred peaks (Fig. S12, ESI†). However, the sol was re-converted to gel state on exposure to the vapor of triethylamine (NEt_3). Triethylamine (Et_3N^+H: pK_a = 10.75) would induce deprotonation of the protonated terpyridine (pK_a < Et_3N^+H),[61] which further coordinate to the respective Eu(III)/Tb(III) ion. FESEM micrographs revealed that actual Eu•L-F-Tb•L-F gel (Fig. 10c) and the corresponding re-converted gel (Fig. 10d) following reversible stimuli conversion possessed almost similar fibrous structures.

View Article Online
DOI: 10.1039/C8TC03487G

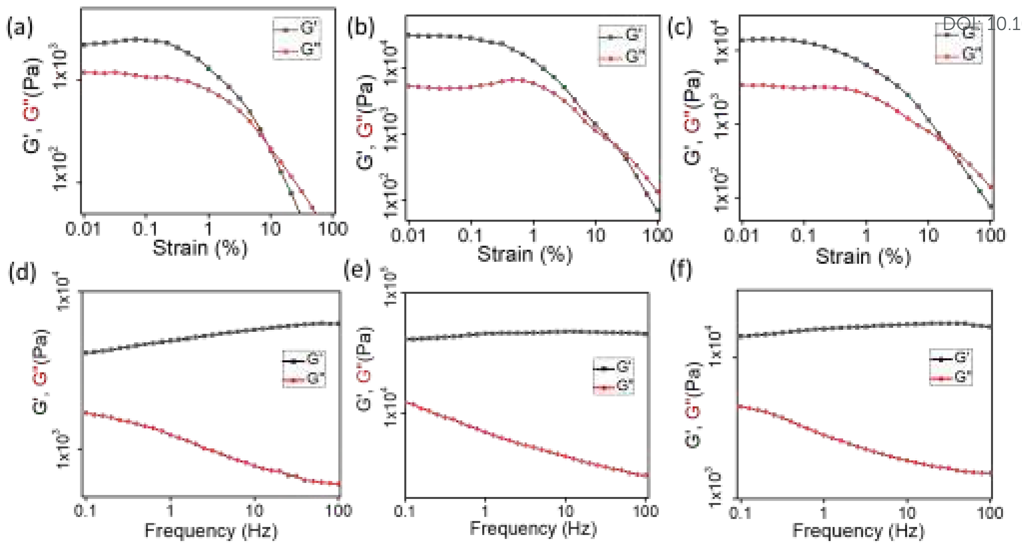

Fig. 9. Oscillatory rheology measurements of L-F, Tb•L-F and Eu•L-F-Tb•L-F gels obtained from DMF. Strain sweeps at frequency = 1 Hz of the storage modulus G' (■) and loss modulus G" (●) for (a) L-F, (b) Tb•L-F and (c) Eu•L-F-Tb•L-F gels. Frequency sweeps at 0.1% strain amplitude for (d) L-F, (e) Tb•L-F and (f) Eu•L-F-Tb•L-F gels

Furthermore, a white-luminescent coating on a silica matrix of a TLC plate (thickness of 0.2 mm, 60 Å pore size, coated on the aluminium plate) was developed by drop-casting a solution of Eu•L-F-Tb•L-F and this was found to be responsive towards pH alteration. The white-luminescent coating was transformed to blue upon exposure to aqueous HCl (pH < 7) due to the protonation of the nitrogen atoms of the terpyridine ligand and subsequent dissociation of Ln–N(terpyridine) coordination bond. Similarly, the white-luminescent coating was altered to blue upon acquaintance to aqueous ammonia solution (pH > 7) as a consequence of the hydrolysis of Ln(III) ions (Fig. 10e).

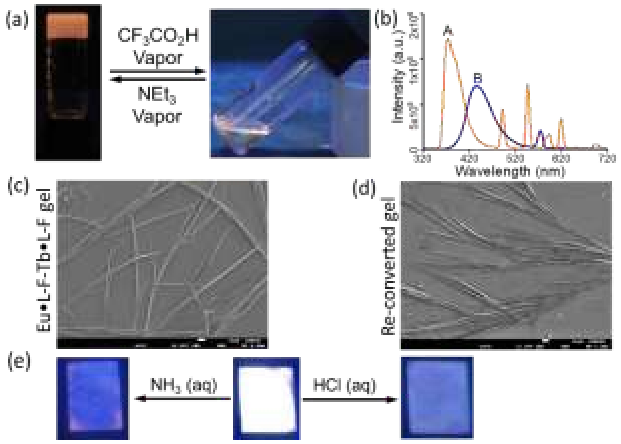

Fig. 10 (a) Stimuli-responsive emission colour changes of Eu•L-F-Tb•L-F gel under UV light, (b) Assessment of luminescence spectra of (A) Eu•L-F-Tb•L-F and (B) TFA exposed Eu•L-F-Tb•L-F sol generated after gel–sol transition, (c and d) FESEM micrographs of Eu•L-F-Tb•L-F gel and the corresponding re-converted gel, (e) White-luminescent coating on a silica matrix of a TLC plate from the Eu•L-F-Tb•L-F and its pH-responsive colour change

Conclusions

In summary, we have demonstrated that the appropriate halo-substituted terpyridine ligands could be used for developing a series of luminescent supramolecular gels with Eu(III), Tb(III), and mixed Eu(III)/Tb(III) or Eu(III)/Ir(III) in DMF solvent. The individual homometallic gels exhibited bright red (Eu-gels) and green (Tb-gels) fluorescence upon exposure to UV light (λ_{ex} = 365 nm). Coordinated terpyridine moiety acted as an antenna by populating the lowest ^5D_J excited state of Eu(III) and Tb(III) through energy transfer and subsequently deactivation to the ^7F_J ground states. Careful tuning of the stoichiometric ratio of Eu(III) and Tb(III) helped in achieving gels that provided various emission colours, including white light. Furthermore, we also perceived near white light emission by doping a blue emissive Ir(III) complex $[Ir^{III}(F_2ppy)_2(biimid)]PF_6$ to the red emissive Eu•L-F/Cl gel. These gel materials can be used to fabricate luminescent agarose gel by simple drop casting procedure and also transparent luminescent PMMA films by incorporating into poly(methyl methacrylate) (PMMA) polymer matrix without altering the optical properties of the metallogels. Moreover, Ln•L-F-PMMA and Eu•L-F-Ir-PMMA films exhibited excellent UV-shielding performance, which is important for developing transparent luminescent PMMA films with excellent UV-shielding properties. Besides, the lanthanide-based gels showed chemo/vapo-chromism based on Ln–N(terpyridine) coordination dynamics, which could offer a suitable pathway for future engineering of stimuli-responsive gel materials.

Experimental section

Materials

All chemicals and solvents used for synthesis were purchased from commercial sources and were used as received without further purification. For spectroscopic measurements and gelation tests HPLC grade solvents were used. 2,2´-biimidazole (biimid)[59] and iridium dimer Tetrakis(4,6-difluorophenyl pyridine-C^2,N')(μ-dichloro)diiridium $[(F_2ppy)_2Ir(\mu\text{-}Cl)]_2$[60] were synthesized following the literature protocols.[59,60]

Instruments

^1H NMR (500 MHz) spectra for the synthesized ligands were recorded on a Bruker AX 500 spectrometer (500 MHz) and was calibrated with respect to the internal standard tetramethylsilane (TMS). Chemical shifts were quantified in ppm with $CDCl_3$ solvent as the internal reference. FT-IR spectra on KBr disks (4000–400 cm^{-1}) were recorded with a Perkin-Elmer 883 spectrometer. High-resolution mass spectra (HRMS) were recorded on Agilent 6545 Q-TOF LC/MS. UV–Vis absorption spectra measurements were performed in 1 cm quartz cuvettes using a Varian Cary 500 spectrometer. Fluorescence spectra were recorded at room temperature using either on a Quanta Master 400, PTI spectrofluorometer or a Fluorolog Horiba Jobin Yvon spectrophotometer.

X-ray diffraction data on appropriate single crystal of L-F were collected on a BRUKER SMART APEX (CCD) diffractometer equipped with a graphite monochromator and Mo-Kα radiation (λ = 0.71073 Å) at 150 K. Data collection and reduction were accomplished using the SMART and SAINT software packages.[62] Multiscan empirical absorption corrections were applied to the data using the program SADABS.[63] The structure was solved by direct methods SHELXTL and was refined on F2 by the full-matrix least-squares technique.[64] Crystallographic data (excluding structure factors) of L-F have been deposited in the Cambridge Crystallographic Data Centre as supplementary publications with CCDC no-1837781

Powder X-ray diffraction (PXRD) patterns were recorded at room temperature on a Philips X'pert X-ray powder diffractometer using Cu-Kα radiation (λ = 1.5418 Å) over 2θ range of 5–50°.

Field emission-scanning electron microscopy (FE-SEM) images were collected using a JEOL JSM-7100F instrument operated at 18 kV accelerating voltage. A small portion of the synthesized gels was scooped out with a spatula and diluted with DMF and the resulting solutions were drop-casted on a silicon wafer and allowed to dry under desiccator for overnight.

Rheological measurements were performed on a Rheoplus MCR302 (Anton Paar) rheometer with parallel plate geometry. After placing the sample, the gap size between the plates was fixed at 0.5 mm. The oscillatory strain sweep measurements were performed at a fixed frequency (f = 1 Hz) by increasing the strain amplitude from 0.1% up to 100% at 25 °C. Frequency sweep measurements were performed from 0.1 to 100 Hz at a fixed small amplitude of strain (0.1%) at 25 °C.

The Fluorescent microscope images were taken using an Olympus BX53 fluorescence microscope.

General procedure for the synthesis of 4′-p-halophenyl-2,2′:6′,2″-terpyridine:

These derivatives were synthesized following previously reported procedures with necessary modification.[50,51] 2-Acetylpyridine (5.42 mL, 48 mmol) was added into the EtOH solution (120 mL) of p-fluoro/chloro-benzaldehyde (24 mmol), followed by addition of KOH pellets (3.70 g, 48 mmol) and aq NH_3 (70 mL, 60 mmol) to the reaction mixture. Further, the reaction mixture was stirred at r.t. for 5 h. The off-white solid generated in due course of the reaction was collected by filtration and washed with EtOH and then dried in a desiccator. The crude material was purified by column chromatography (silica gel, CH_2Cl_2: MeOH, 97:3) to obtain pure ligands as an off-white solid. Detailed characterization of L-F and L-Cl are provided in the supporting information (Page 2, ESI).

L-X gel formation

A weighted amount of L-X (4.9×10^{-2} M) (X = F and Cl) was added to MeCN (1 mL) and sonicated for 2-3 min followed by heating till the clear solutions obtained, which eventually resulted in stable white opaque gels upon cooling to room temperature within 2-5 h. The gel formation was confirmed by an inverted vial method. Gelation was also found in DMF and mixed solvent MeCN/DMF (1:1, v/v).

Formation of Eu•L-X and Tb•L-X gels

To the DMF solution of L-X (X = F and Cl; 6.25×10^{-2} M, 500 μL), 500 μL DMF solution of $Eu(NO_3)_3{\cdot}6H_2O$ or $Tb(NO_3)_3{\cdot}6H_2O$ (6.25×10^{-2} M, 500 μL) were mixed and the mixture was sonicated and heated until the clear solutions attained. Next, the solutions were left undisturbed for few hours at ambient temperature resulted in a stable metallogel of Eu•L-X and Tb•L-X, which were stable upon inversion of the vials.

Selected FTIR bands: (KBr, cm^{-1}, vs = very strong, br = broad, s = strong and m = medium) Eu•L-F: 3422 (br), 1650 (s), 1608 (s), 1583 (s), 1513 (vs), 1465 (m), 1382 (vs), 1225 (m), 1162 (m), 832 (s), 786 (vs), 732 (s).

Tb•L-F: 3420 (br), 1651 (s), 1606 (s), 1510 (s), 1466 (m), 1382 (vs), 1228 (m), 1164 (m), 834 (m), 786 (s), 734 (m).

Formation of mixed-metallic Eu•L-X-Tb•L-X, Eu•L-X-2(Tb•L-X) and Eu•L-X-Ir gels (X = F, Cl)

Mixed-metallic Eu•L-X-Tb•L-X gels were prepared by mixing $Eu(NO_3)_3{\cdot}6H_2O$ (6.25×10^{-2} M, 250 μL) and $Tb(NO_3)_3{\cdot}6H_2O$ (6.25×10^{-2} M, 250 μL) to L-X (6.25×10^{-2} M, 500 μL) in DMF solvent. Similarly, Eu•L-X-2(Tb•L-X) gels were synthesized by mixing $Eu(NO_3)_3{\cdot}6H_2O$ (2.08×10^{-2} M, 250 μL) and $Tb(NO_3)_3{\cdot}6H_2O$ (4.17×10^{-2} M, 250 μL) to 500 μL solution of L-X (6.25×10^{-2} M) in DMF solvent.

Eu•L-X-Ir gels were obtained by adding a weighted amount (16 mg) of the Ir(III) complex $[Ir^{III}(F_2ppy)_2(biimid)]PF_6$ into the Eu•L-X sol (6.25×10^{-2} M, 1mL).

In all the cases, the formation of gels was confirmed by inversion test methodology.

Preparation of $[Ir^{III}(F_2ppy)_2(biimid)]PF_6$

The complex was synthesized following a literature procedure with slight modifications.[58] A 0.84 mmol (2.4 equiv) amount of 2,2′-biimidazole (biimid)[59] was added to the ethanolic solution (10 mL) iridium dimer $[(F_2ppy)_2Ir(\mu\text{-}Cl)]_2$[60] (0.35 mmol (1 equiv)) and the reaction mixture was refluxed for 16 h under nitrogen. After cooling to ambient temperature, a saturated aqueous of KPF_6 (3 mmol, 0.48 gm) was added with stirring and the solution was stirred for 30 min. The appeared precipitate was filtered off using a glass frit and washed with cold methanol and water for further purification and then dried in a desiccator. Yield: 0.32 gm, 38%. ^1H NMR (600 MHz, $CDCl_3$) δ 13.27 (s, 2H), 8.25 (d, J = 8.5 Hz, 2H), 7.76 (t, J = 7.8 Hz, 2H), 7.64 (t, J = 10.2 Hz, 2H), 7.15 (d, J = 17.8 Hz, 2H), 7.03 (t, J = 6.6 Hz, 2H), 6.57 – 6.36 (m, 4H), 5.76 (dd, J = 8.5, 2.0 Hz, 2H). HRMS (ESI): calcd for $C_{28}H_{18}N_6F_4Ir$ $[M]^+$ 707.1158 found 707.1203.

View Article Online
DOI: 10.1039/C8TC03487G

Conflicts of interest

There are no conflicts to declare.

Acknowledgments

T.S.M. acknowledge SERB (India) Grant PDF/2016/002461 for funding and fellowship. A. D. acknowledges SERB (India) (EMR/2016/001850, & JCB/2017/000004) and DRDO (ERIP/ER/1502249/M/01) Grants for funding. SKP acknowledges Grant SERB (PDF/2015/000745) for funding and fellowship. Authors acknowledge Dr. Suresh K. Jewrajka (CSIR-CSMCRI) for providing us the poly(methyl methacrylate) (PMMA) for our experiments.

References

1 A. R. Hirst, B. Escuder, J. F. Miravet and D. K. Smith, *Angew. Chem., Int. Ed.*, 2008, **47**, 8002-8018.
2 P. Chen, Q. Li, S. Grindy and N. Holten-Andersen, *J. Am. Chem. Soc.*, 2015, **137**, 11590-11593.
3 J. A. Foster, K. K. Damodaran, A. Maurin, G. M. Day, H. P. G. Thompson, G. J. Cameron, J. C. Bernal and J. W. Steed, *Chem. Sci.*, 2017, **8**, 78-84.
4 J. A. Foster, M.-O. M. Piepenbrock, G. O. Lloyd, N. Clarke, J. A. K. Howard and J. W. Steed, *Nat. Chem.*, 2010, **2**, 1037.
5 P. Dastidar, *Chem. Soc. Rev*, 2008, **37**, 2699-2715.
6 A. Maity, F. Ali, H. Agarwalla, B. Anothumakkool and A. Das, *Chem. Commun.*, 2015, **51**, 2130-2133.
7 Z. Yang, G. Liang and B. Xu, *Acc. Chem. Res.*, 2008, **41**, 315-326.
8 Y. Zhou, H.-Y. Zhang, Z.-Y. Zhang and Y. Liu, *J. Am. Chem. Soc.*, 2017, **139**, 7168-7171.
9 A. Y.-Y. Tam and V. W.-W. Yam, *Chem. Soc. Rev*, 2013, **42**, 1540-1567.
10 J. W. Steed, *Chem. Soc. Rev*, 2010, **39**, 3686-3699.
11 V. K. Praveen, C. Ranjith and N. Armaroli, *Angew. Chem., Int. Ed.*, 2014, **53**, 365-368.
12 S. S. Babu, V. K. Praveen and A. Ajayaghosh, *Chem. Rev*, 2014, **114**, 1973-2129.
13 G. Yu, X. Yan, C. Han and F. Huang, *Chem. Soc. Rev*, 2013, **42**, 6697-6722.
14 S. Y.-L. Leung, S. Evariste, C. Lescop, M. Hissler and V. W.-W. Yam, *Chem. Sci.*, 2017, **8**, 4264-4273.
15 A. Harada, R. Kobayashi, Y. Takashima, A. Hashidzume and H. Yamaguchi, *Nat. Chem.*, 2010, **3**, 34.
16 A. Sorrenti, R. Rodriguez-Trujillo, D. B. Amabilino and J. Puigmartí-Luis, *J. Am. Chem. Soc.*, 2016, **138**, 6920-6923.
17 J. R. Moffat, G. J. Seeley, J. T. Carter, A. Burgess and D. K. Smith, *Chem. Commun.*, 2008, 4601-4603.
18 M. Martínez-Calvo, O. Kotova, M. E. Möbius, A. P. Bell, T. McCabe, J. J. Boland and T. Gunnlaugsson, *J. Am. Chem. Soc.*, 2015, **137**, 1983-1992.
19 K. Oxana, D. Ronan, d. S. C. M. G., B. Markus, K. P. E., B. J. J. and G. Thorfinnur, *Angew. Chem., Int. Ed.*, 2012, **51**, 7208-7212.
20 D. E. Barry, D. F. Caffrey and T. Gunnlaugsson, *Chem. Soc. Rev*, 2016, **45**, 3244-3274.
21 G. Tumpa and U. Maitra, *Angew. Chem., Int. Ed.*, 2017, **56**, 10730-10734.
22 S. Banerjee, R. Kandanelli, S. Bhowmik and U. Maitra, *Soft Matter*, 2011, **7**, 8207-8215.
23 P. Sutar, V. M. Suresh and T. K. Maji, *Chem. Commun.*, 2015, **51**, 9876-9879.
24 P. Sutar and T. K. Maji, *Inorg. Chem.*, 2017, **56**, 9417-9425.
25 C. Kim, K. Y. Kim, J. H. Lee, J. Ahn, K. Sakurai, S. S. Lee and J. H. Jung, *ACS Appl. Mater. Interfaces*, 2017, **9**, 3799-3807.
26 W. K.-L., L. G.-L., Y. Y.-Y. and W. W.-T., *Adv. Mater.*, 2006, **18**, 1051-1054.
27 P. Sutar and T. K. Maji, *Chem. Commun.*, 2016, **52**, 8055-8074.
28 S. Mohapatra, S. Adhikari, H. Riju and T. K. Maji, *Inorg. Chem.*, 2012, **51**, 4891-4893.
29 W.-X. Feng, S.-Y. Yin, M. Pan, H.-P. Wang, Y.-N. Fan, X.-Q. Lü and C.-Y. Su, *J. Mater. Chem. C*, 2017, **5**, 1742-1750.
30 P. Kumar, S. Soumya and E. Prasad, *ACS Appl. Mater. Interfaces*, 2016, **8**, 8068-8075.
31 P. Coppo, M. Duati, V. N. Kozhevnikov, J. W. Hofstraat and L. D. Cola, *Angew. Chem., Int. Ed.*, 2005, **44**, 1806-1810.
32 D. Sykes, I. S. Tidmarsh, A. Barbieri, I. V. Sazanovich, J. A. Weinstein and M. D. Ward, *Inorg. Chem.*, 2011, **50**, 11323-11339.
33 D. Sykes, S. C. Parker, I. V. Sazanovich, A. Stephenson, J. A. Weinstein and M. D. Ward, *Inorg. Chem.*, 2013, **52**, 10500-10511.
34 J. A. Kaplan, P. Barthelemy and M. W. Grinstaff, *Chem. Commun.*, 2016, **52**, 5860-5863.
35 C. Giansante, G. Raffy, C. Schäfer, H. Rahma, M.-T. Kao, A. G. L. Olive and A. Del Guerzo, *J. Am. Chem. Soc.*, 2011, **133**, 316-325.
36 J. F. Galisteo-Lopez, S. Gomez-Esteban, B. Gomez-Lor and C. Lopez, *J. Mater. Chem. C*, 2015, **3**, 5764-5768.
37 L. Yongguang, W. K. Man-Chung, T. A. Yiu-Yan, W. Lixin and Y. V. Wing-Wah, *Chem. Eur. J*, 2010, **16**, 8690-8698.
38 J. Y. R. Silva, L. L. da Luz, F. G. M. Mauricio, I. B. Vasconcelos Alves, J. N. d. S. Ferro, E. Barreto, I. T. Weber, W. M. de Azevedo and S. A. Júnior, *ACS Appl. Mater. Interfaces*, 2017, **9**, 16458-16465.
39 Y. Cui, H. Xu, Y. Yue, Z. Guo, J. Yu, Z. Chen, J. Gao, Y. Yang, G. Qian and B. Chen, *J. Am. Chem. Soc.*, 2012, **134**, 3979-3982.
40 D. Ananias, F. A. A. Paz, D. S. Yufit, L. D. Carlos and J. Rocha, *J. Am. Chem. Soc.*, 2015, **137**, 3051-3058.
41 A. J. McConnell, C. S. Wood, P. P. Neelakandan and J. R. Nitschke, *Chem. Rev*, 2015, **115**, 7729-7793.
42 Y. Sagara and T. Kato, *Nat. Chem.*, 2009, **1**, 605.
43 J. H. v. Esch and B. L. Feringa, *Angew. Chem., Int. Ed.*, 2000, **39**, 2263-2266.
44 S. Yagai, T. Nakajima, K. Kishikawa, S. Kohmoto, T. Karatsu and A. Kitamura, *J. Am. Chem. Soc.*, 2005, **127**, 11134-11139.
45 S.-k. Ahn, R. M. Kasi, S.-C. Kim, N. Sharma and Y. Zhou, *Soft Matter*, 2008, **4**, 1151-1157.
46 T. Z. Grove, C. O. Osuji, J. D. Forster, E. R. Dufresne and L. Regan, *J. Am. Chem. Soc.*, 2010, **132**, 14024-14026.
47 P. T. Mather, *Nat. Mater.*, 2007, **6**, 93.
48 Q. Zhu, L. Zhang, K. Van Vliet, A. Miserez and N. Holten-Andersen, *ACS Appl. Mater. Interfaces*, 2018, **10**, 10409-10418.
49 M. C. Heffern, L. M. Matosziuk and T. J. Meade, *Chem. Rev*, 2014, **114**, 4496-4539.
50 J. Wang and G. S. Hanan, *Synlett*, 2005, **2005**, 1251-1254.
51 A. Maron, A. Szlapa, T. Klemens, S. Kula, B. Machura, S. Krompiec, J. G. Malecki, A. Switlicka-Olszewska, K. Erfurt and A. Chrobok, *Org. Biomol. Chem*, 2016, **14**, 3793-3808.
52 H. Agarwalla, K. Jana, A. Maity, M. K. Kesharwani, B. Ganguly and A. Das, *J. Phys. Chem. A.*, 2014, **118**, 2656-2666.
53 T. S. Mahapatra, S. Chaudhury, S. Dasgupta, V. Bertolasi and D. Ray, *New J. Chem.*, 2016, **40**, 2268-2279.
54 S. Petoud, J.-C. G. Bünzli, K. J. Schenk and C. Piguet, *Inorg. Chem.*, 1997, **36**, 1345-1353.
55 K. Sénéchal-David, A. Hemeryck, N. Tancrez, L. Toupet, J. A. G. Williams, I. Ledoux, J. Zyss, A. Boucekkine, J.-P. Guégan, H. Le Bozec and O. Maury, *J. Am. Chem. Soc.*, 2006, **128**, 12243-12255.

View Article Online
DOI: 10.1039/C8TC03487G

56 B. Ahrens, S. A. Cotton, N. Feeder, O. E. Noy, P. R. Raithby and S. J. Teat, *J. Chem. Soc., Dalton Trans.*, 2002, 2027-2030.

57 H. Nozary, C. Piguet, P. Tissot, G. Bernardinelli, J.-C. G. Bünzli, R. Deschenaux and D. Guillon, *J. Am. Chem. Soc.*, 1998, **120**, 12274-12288.

58 J. C. Freys, G. Bernardinelli and O. S. Wenger, *Chem. Commun.*, 2008, DOI: 10.1039/B806175K, 4267-4269.

59 J.-C. Xiao and J. n. M. Shreeve, *J. Org. Chem.*, 2005, **70**, 3072-3078.

60 S. Sprouse, K. A. King, P. J. Spellane and R. J. Watts, *J. Am. Chem. Soc.*, 1984, **106**, 6647-6653.

61 K. L. Cheng, K. Ueno, T. Imamura, *CRC Handbook of Organic Analytical Reagents,* 2nd ed., CRC Press, Florida, 1992**.**

62 G. M. Sheldrick, *SAINT 5.1 ed.*; Siemens Industrial Automation Inc., Madison, WI, 1995.

63 *SADABS, Empirical Absorption Correction Program*; University of Göttingen, Göttingen, Germany, 1997.

64 G. M. Sheldrick, *SHELXTL Reference Manual: Version 5.1*; Bruker AXS, Madison, WI, 1997.

View Article Online
DOI: 10.1039/C8TC03487G

Table of contents:

Text:

Lanthanide-based light-emitting supramolecular thermoreversible metallogels with tunable luminescence by controlling the stoichiometry of L-X/Eu^{III}•L-X/Tb^{III}•L-X or L-X/Eu^{III}•L-X/[Ir^{III}(F$_2$ppy)$_2$(biimid)]PF$_6$.

Graphic: